



**HAL**  
open science

## Identification of small molecules disrupting the ubiquitin proteasome system in malaria Running title: Inhibition of *P. falciparum* Ubiquitin Proteasome System

Lydia Mata-Cantero, María Jesús Chaparro, Gonzalo Colmenarejo, Concepción Cid, Álvaro Cortés, Manuel S Rodriguez, Julio Martín, F Javier Gamo, Maria G Gomez- Lorenzo

### ► To cite this version:

Lydia Mata-Cantero, María Jesús Chaparro, Gonzalo Colmenarejo, Concepción Cid, Álvaro Cortés, et al.. Identification of small molecules disrupting the ubiquitin proteasome system in malaria Running title: Inhibition of *P. falciparum* Ubiquitin Proteasome System. *ACS Infectious Diseases*, 2019, 5 (12), pp.2105-2117. 10.1021/acsinfecdis.9b00216 . hal-03023985

**HAL Id: hal-03023985**

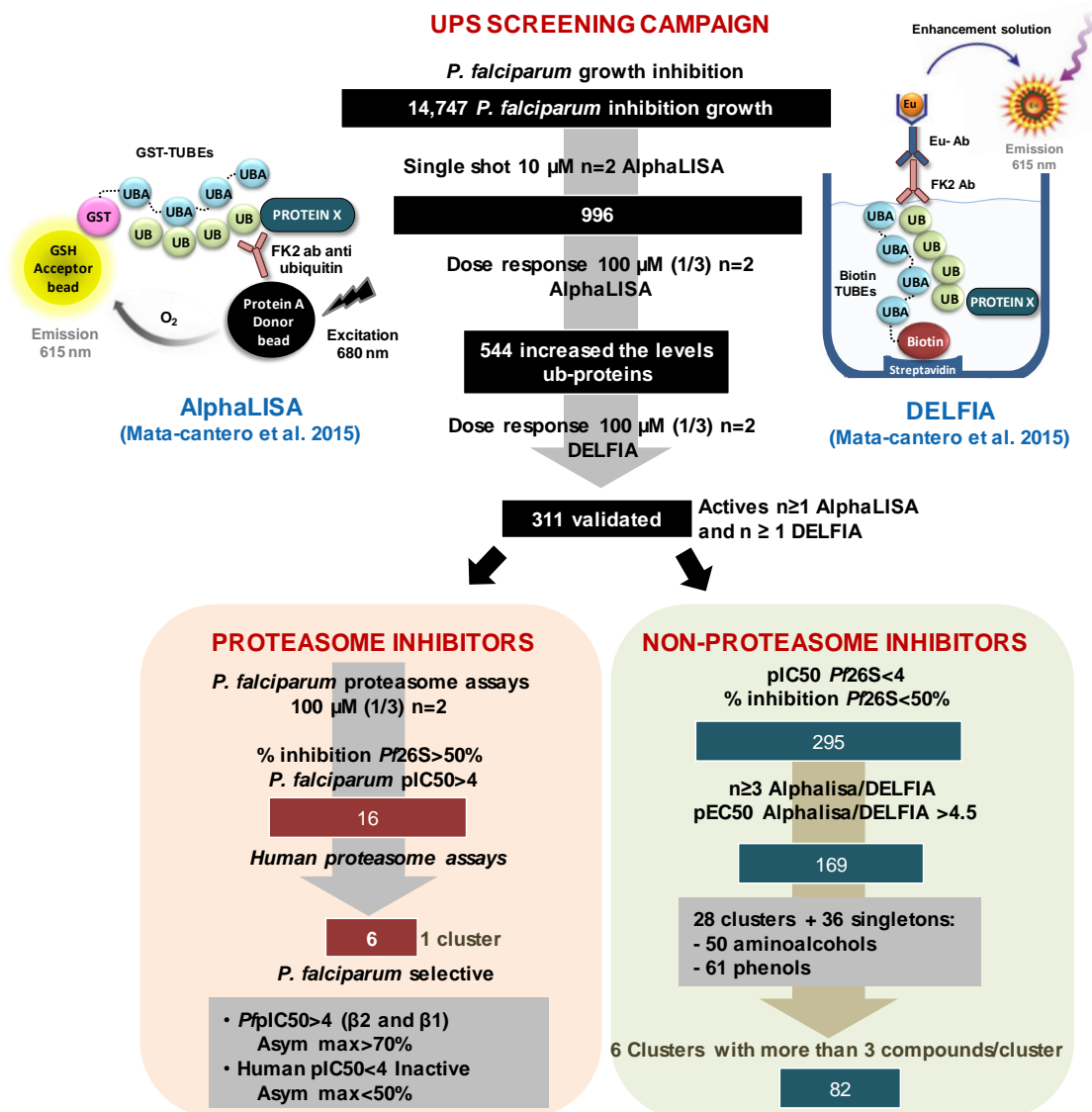
**<https://hal.science/hal-03023985>**

Submitted on 25 Nov 2020

**HAL** is a multi-disciplinary open access archive for the deposit and dissemination of scientific research documents, whether they are published or not. The documents may come from teaching and research institutions in France or abroad, or from public or private research centers.

L'archive ouverte pluridisciplinaire **HAL**, est destinée au dépôt et à la diffusion de documents scientifiques de niveau recherche, publiés ou non, émanant des établissements d'enseignement et de recherche français ou étrangers, des laboratoires publics ou privés.





32

33

34 **Abstract**

35

36 The Ubiquitin Proteasome System (UPS) is one of the main proteolytic pathways in  
 37 eukaryotic cells, playing an essential role in key cellular processes such as cell cycling and signal  
 38 transduction. Changes in some of the components of this pathway have been implicated in  
 39 various conditions, including cancer and infectious diseases such as malaria. The success of  
 40 therapies based on proteasome inhibitors has been shown in human clinical trials. In addition to  
 41 its proven tractability, the essentiality of the *Plasmodium falciparum* UPS underlines its potential  
 42 as a source of targets to identify new antimalarial treatments. Two assays, previously developed

43 to quantify the parasite protein ubiquitylation levels in a high throughput format, have been used  
44 to identify compounds that inhibit parasite growth by targeting *P. falciparum* UPS. Among the  
45 positive hits, specific inhibitors of the *P. falciparum* proteasome have been identified and  
46 characterized. Hits identified using this approach may be used as starting points for development  
47 of new antimalarial drugs. They may also be used as tools to further understand proteasome  
48 function, and to identify new targets in *P. falciparum* UPS.

49

## 50 **Abbreviations**

51 UPS, ubiquitin proteasome system; DUB, deubiquitinase; TUBEs, tandem ubiquitin binding  
52 entities; UBA, ubiquitin-associated domains; iRBCs, infected red blood cells; HTS, high  
53 throughput screening; S/B, signal to background; CV, coefficient of variation; SD, standard  
54 deviation; Ub, ubiquitin; TCAMs, Tres Cantos antimalarial Set; PFI, Property Forecast Index; IFI,  
55 Inhibition Frequency Index; ACTs, artemisinin combination therapies; NA, non-adjusted

56

## 57 **Keywords**

58 *Plasmodium falciparum*, proteasome, UPS, inhibitor, screening, ubiquitylation

59

## 60 **Introduction**

61

62 The most severe form of malaria is caused by the protozoan parasite *Plasmodium*  
63 *falciparum*. This disease is one of the deadliest infectious diseases in the world, causing more  
64 than 400,000 deaths per year (1). Current first-line treatment is based on artemisinin combination  
65 therapies (ACTs). However, the malaria parasite has developed resistance against all widely used  
66 antimalarials, and ACTs are not an exception. Increasing drug resistance has led to an urgent  
67 need for developing new therapies effective not only on acute infection with high parasite loads  
68 in blood, but also on different stages of the parasite to block transmission. Thus, identification of  
69 drugs targeting different mechanisms in different stages of the parasite is crucial for malaria  
70 eradication (2).

71 In recent years, *P. falciparum* ubiquitin proteasome system (UPS) has been considered a  
72 promising target for drug development (3, 4). Ubiquitylation is a post-translational change in which  
73 ubiquitin (Ub) is covalently bound to the target protein. This process requires the sequential action  
74 of three groups of enzymes, E1 ubiquitin-activating enzymes, E2 ubiquitin-conjugating enzymes,  
75 and E3 ligases. E3 ligases are the main responsible for substrate specificity leading to the transfer  
76 of ubiquitin from the E2 ligase to the final substrate. This ubiquitylation process can also be  
77 reverted by the action of deubiquitylation enzymes (DUBs). The cooperative interplay between  
78 the ubiquitylation and deubiquitylation processes determines the prevalence of certain  
79 ubiquitylated proteins in the cell and, thus, the activation/deactivation of specific functions (5).

80 Eukaryotic 26S proteasome consists of a 20S core, responsible for catalytic activity, and two  
81 regulatory 19S particles located at both sides that control entry of ubiquitylated proteins into the  
82 proteolytic core. 20S comprises four heptameric rings, of which the outer rings are formed by  
83 alpha subunits and the inner rings by catalytic beta subunits,  $\beta$ 1 (caspase-like),  $\beta$ 2 (trypsin-like)  
84 and  $\beta$ 5 (chymotrypsin-like) (6).

85 UPS controls key processes in eukaryotic cells including apoptosis, cell cycle and DNA  
86 repair. Thus, UPS deregulation has been related to multiple diseases such as cancer,  
87 neurological disorders, and pathogen infections (7). In 2003, the proteasome inhibitor bortezomib  
88 was the first drug within the UPS approved by the US Food and Drug Administration for the  
89 treatment of multiple myeloma. Several UPS inhibitors have subsequently been launched or  
90 tested in clinical trials (8, 9).

91 In addition to its proven tractability as drug target, different studies have revealed the  
92 essentiality of *P. falciparum* UPS in its survival and transmission (10, 11). Irreversible inhibition of  
93 parasite growth on all parasite stages has been seen using different types of human proteasome  
94 inhibitors, some of them within the nanomolar range (3). Moreover, they also show a synergistic  
95 behavior in resistant parasites when combined with artemisinin (3, 12). While *P. falciparum*  
96 proteasome exhibits a high degree of homology with its human counterpart, some divergences  
97 have been found in the  $\beta$ 2 active site by cryo-electron microscopy (12, 13). These divergences  
98 are being exploited to develop inhibitors with selectivity for the parasite proteasome to avoid side  
99 effects (12-14).

100 On the other hand, most studies of *P. falciparum* UPS are focused on the *P. falciparum*  
101 proteasome remaining the UPS upstream components understudied. Although all the main UPS  
102 components have been identified in the parasite genome *in silico*, only some of them have been  
103 tested experimentally (15, 16). While E1 and E2 paralogs are highly conserved, E3 ligases and  
104 DUBs are highly divergent, thus offering the possibility to develop selective drugs.

105 The objective of this study was to identify inhibitors with potential to interfere with any of the  
106 steps involved in the parasite UPS. For that, two previously reported cellular assays that  
107 quantitatively measure changes in ubiquitylated protein levels (17) were used. As a key  
108 advantage, these methods do not require extensive or previous knowledge of the targets they are  
109 hitting. A high throughput screening (HTS) campaign was run with the Tres Cantos AntiMalarial  
110 Set (TCAMS), a GSK compound collection of ca 13K compounds that inhibits *P. falciparum in*  
111 *vitro* growth (18). As a result, we were able to identify new chemical entities that inhibit the parasite  
112 proteasome, validating the approach used. Moreover, compounds acting through other  
113 components of the parasite UPS were also identified. All these hits can be followed up to develop  
114 new antimalarial drugs with novel modes of action.

115

## 116 **Results and discussion**

117

### 118 ***High throughput screening at single shot with AlphaLISA assay***

119

120 Two cellular assays previously developed were used to run an HTS campaign (17).  
121 Progression cascade of the whole HTS can be found in the graphical abstract. In both assays,  
122 the signal measured is proportional to the amount of ubiquitylated proteins amount present in *P.*  
123 *falciparum* cells, allowing the identification of UPS inhibitors that are able to change the total levels  
124 of ubiquitylated proteins in cells.

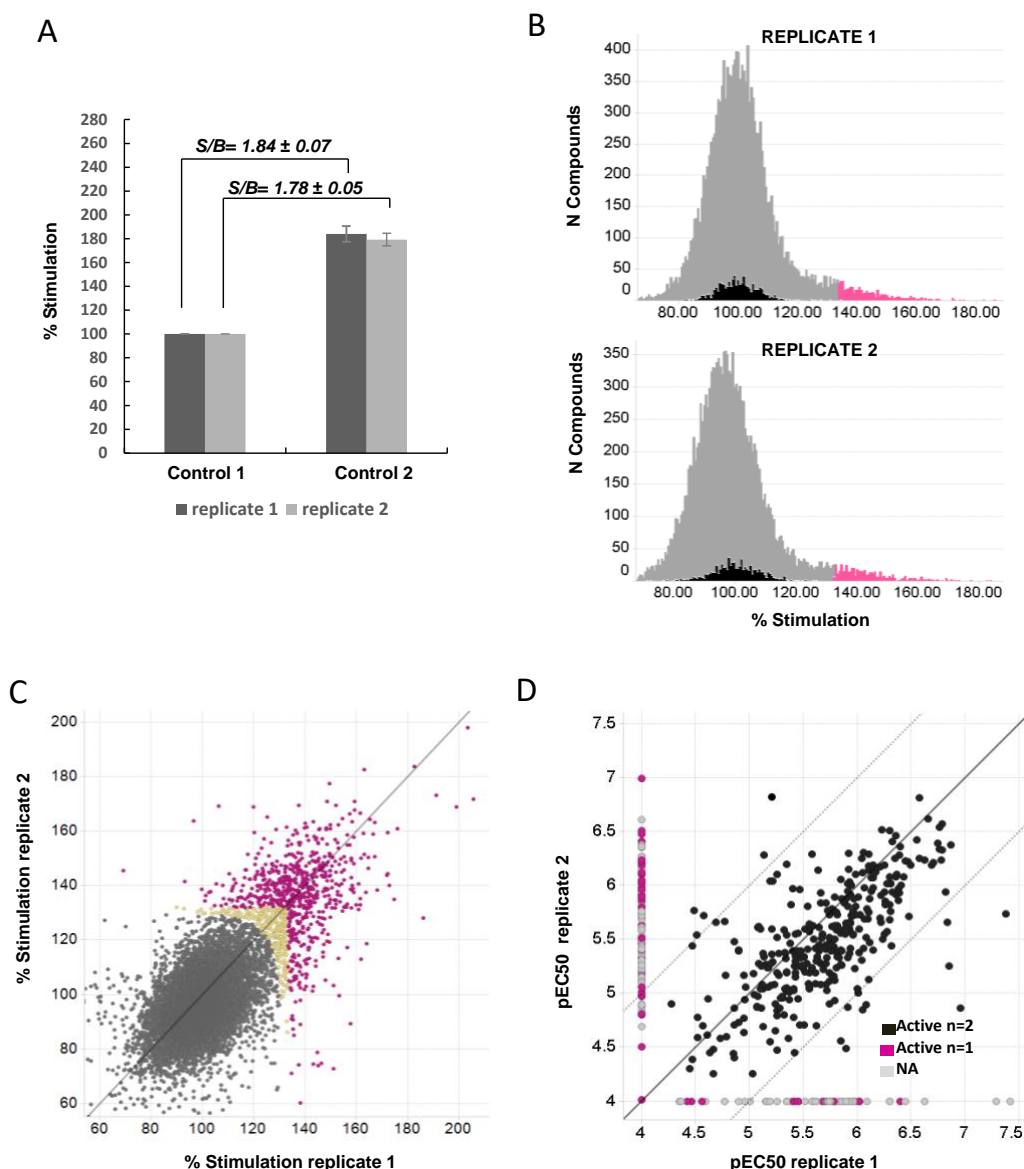
125 The homogeneous AlphaLISA assay was selected to perform the primary screening  
126 campaign, as it can be run in 1536-well plates and requires no washing steps. AlphaLISA is a  
127 cellular assay where compounds are incubated with infected red blood cells (iRBCs) for 1 hour.  
128 This time of incubation was chosen to rule out that the changes measured in the total pool of

129 ubiquitylated protein after treatment are the result of the effect of the compound on other pathways  
130 instead of on the UPS.

131 As the assay is cell-based the selected compound collection consisted of the TCAM set (18)  
132 and other compounds from the GlaxoSmithKline HTS screening collection which inhibited *P.*  
133 *falciparum in vitro* growth in previous whole cell phenotypic screenings. A total of 14,747  
134 compounds were tested. The aim was to identify compounds that inhibit parasite growth through  
135 the UPS, as the mechanisms of action of most compounds in this collection set remain unknown.

136 Assay was performed in duplicate at a final assay concentration of 10  $\mu$ M. Two controls per  
137 plate were used: Control 1, samples in absence of compounds (basal levels of ubiquitylated  
138 proteins in the cell) and Control 2, samples in presence of proteasome inhibitor MG132 at a  
139 concentration that produces complete proteasome inhibition (19). The AlphaLISA signal obtained  
140 for each compound was normalized as percent stimulation compared to Control 1, corresponding  
141 to 100% stimulation. Control 2 was not used to normalize the percent inhibition of each compound  
142 because the levels of ubiquitylated protein accumulation could vary depending on the target  
143 affected within the UPS. MG132 increased ubiquitylated protein levels in the cells approximately  
144 1.8 times as compared to Control 1 (Figure 1A) (180% stimulation) and was used to control the  
145 assay performance for each plate, that was in the range of previously reported data (17).

146 Patterns in plate responses were corrected using an in-house developed algorithm (20). The  
147 percentage of stimulation found for the compounds followed a normal distribution in both  
148 replicates (Figure 1B). Most compounds and Control 1 samples showed a percentage of  
149 stimulation centered around 100% (inactive compounds). The right tail in pink correspond to the  
150 actives hits of the assay. These compounds have a percentage of stimulation above the robust  
151 cut-off in at least one of the replicates. Robust cut-off was estimated through a robust algorithm  
152 (21) that considers the mean value of Control 1 plus three times its standard deviation. The  
153 resulting cut-offs for both replicates were very similar (132% and 133% for replicates 1 and 2  
154 respectively). Figure 1C shows the correlation of the percentage stimulation between both  
155 replicates. In addition, a Pareto ranking was calculated with the two responses, to estimate a  
156 round cut-off for this bivariate distribution. Compounds labeled in yellow are the ones rescued in  
157 this way, giving a total hit rate of 6.8% of all compounds tested.



158  
 159  
 160  
 161  
 162  
 163  
 164  
 165  
 166  
 167  
 168  
 169  
 170  
 171  
 172  
 173  
 174  
 175  
 176  
 177  
 178  
 179  
 180

**Figure 1. AlphaLISA screening campaign.** Compounds were tested in the AlphaLISA assay in duplicate at 10  $\mu$ M. Two controls per plate were included and normalized as percent stimulation. Control 1 corresponded to the signal obtained in absence of inhibition (basal levels of ubiquitylated proteins corresponding to 100%), while Control 2 was the signal measured in wells treated with the proteasome inhibitor MG132 (1.5  $\mu$ M). **A.** Bars represent the average percent stimulation for each control in the replicates. Average signal to background obtained per plate ( $S/B = \text{Average \% stimulation control 2 wells} / \text{Average \% stimulation control 1 wells}$ ) is given in bold for each replicate. **B.** Number of wells for a given percent stimulation. All compounds tested (14,747) plus control 1 wells are represented. Black color corresponds to control 1 wells, while wells treated with compounds appear in grey. Compounds with percent stimulation above the statistical cut-off for each replicate being considered active hits are depicted in pink. **C.** Correlation of the percent stimulation obtained for each replicate. Inactive compounds are colored grey, and active hits in at least one replicate are labeled in pink as in B. Yellow compounds were rescued after calculating a Pareto round cut-off. The line indicates the perfect correlation ( $y=x$ ). **D.** Active hits were then assayed at dose response starting at 100  $\mu$ M (1:3 dilutions) per duplicate. Graph shows the correlation of the pEC50s obtained for each replicate. Compounds displaying a maximum percent stimulation higher than 131% were considered active compounds. Actives in two replicates ( $n=2$ ) are represented in black, those active in one replicate and inactive in the other one in pink ( $n=1$ ), and actives in one replicate but whose curves could not be fitted (non-adjusted NA) in the other replicate appear in grey. The black line is the perfect correlation ( $y=x$ ), while dotted lines represent  $\pm 1$  log difference of perfect correlation.



181  
182 A total of 996 compounds were considered actives in at least one of the replicates. They  
183 were progressed to dose response experiments to determine their potency. The quality of the  
184 assay was assessed with different proteasome inhibitor being in the range of previously reported  
185 data (17) (Table 1). The minimum percentage of stimulation considered out of the noise of the  
186 assay was 131%, because this corresponded to the statistical cut-off in both replicates.  
187 Compounds displaying curves with a maximal asymptote above this percent stimulation in at least  
188 one replicate were considered active compounds. Thus, 544 compounds met these criteria, giving  
189 a confirmation rate of 54.6%.

190 Figure 1D depicts the correlation between pEC50s obtained per replicate. 438 compounds  
191 were positive in both replicates, showing a pEC50 correlation within the range of  $pEC50_{\text{replicateX}} -$   
192  $pEC50_{\text{replicateZ}} < 1$ , represented by grey dotted lines. The other 106 compounds were active in one  
193 of the replicates, while in the other replicate they were inactive ( $pEC50 < 4$ , pink) or could not be  
194 fitted with the analysis software due to variability (grey, non-adjusted, NA).

195

#### 196 ***Hit confirmation with DELFIA assay***

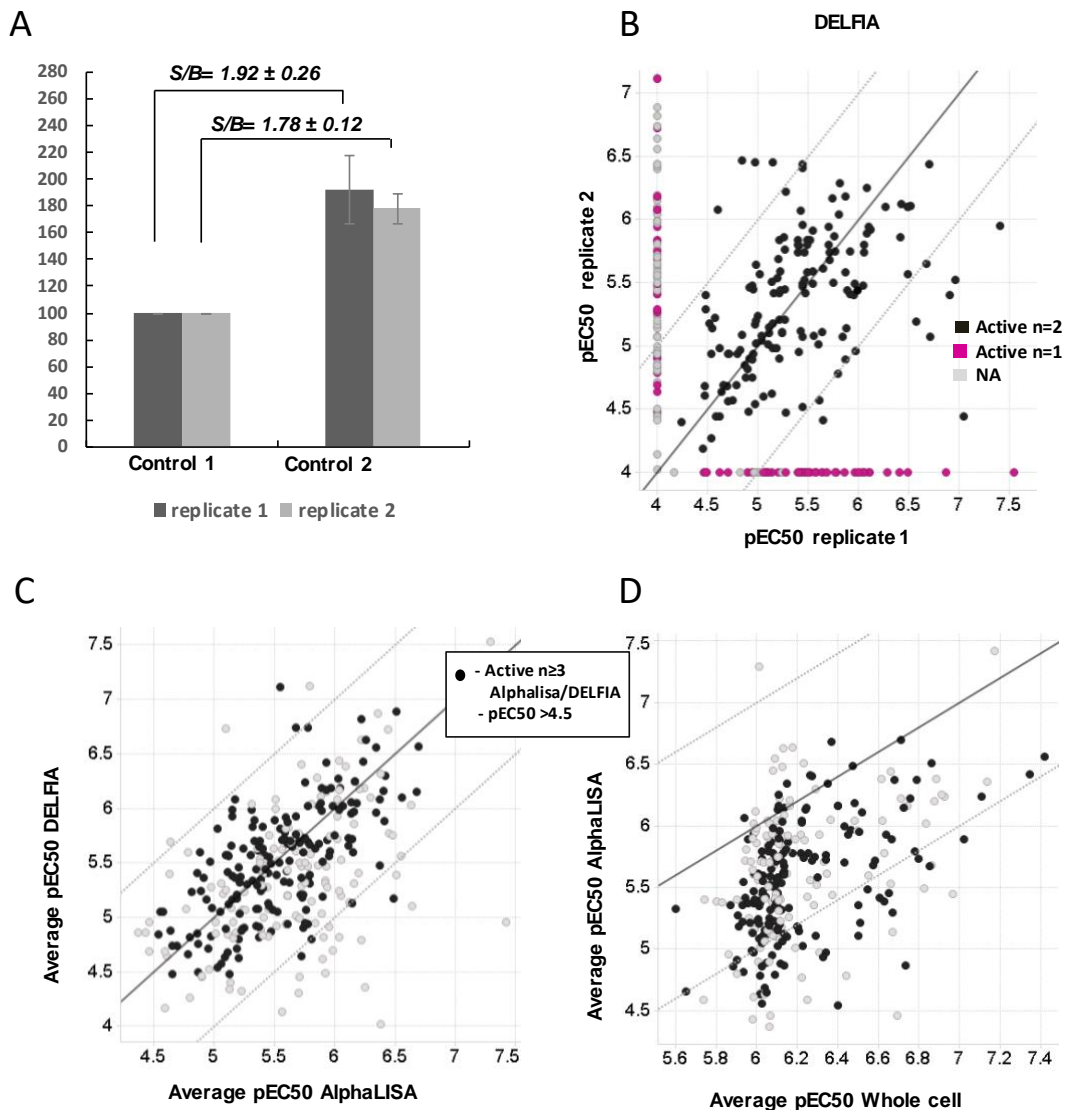
197

198 Hits from the AlphaLISA assay were further tested in the orthogonal DELFIA assay (17). This  
199 heterogeneous assay was performed to confirm the effect of the hits on the UPS and to rule out  
200 non-specific interference in the AlphaLISA assay as washes are performed between each  
201 addition step.

202 Hits from the AlphaLISA assay (544 compounds) were tested at dose response per duplicate  
203 (Figure 2). Assay behavior was similar to that of AlphaLISA in terms of signal to background and  
204 cut-off. The results of the DELFIA assay showed a greater variability in replicates due to the  
205 extensive washing steps but, at the same time, the stringent conditions allowed for robust  
206 validation of the inhibitors found in the primary screening with the AlphaLISA assay.

207 Presence of the proteasome inhibitor MG132 led to increase ubiquitylated protein levels up  
208 to 185%, (Figure 2A). Compounds with a maximum asymptote higher than 131% were active  
209 (robust cut-off). Figure 2B shows the correlation of the pEC50s obtained between DELFIA  
210 replicates. Only 106 hits were active in both replicates. Curves from many compounds could not

211 be fitted in one of the replicates due to assay variability or because they were close to the  
 212 response background (labeled as NA in Figure 2B).

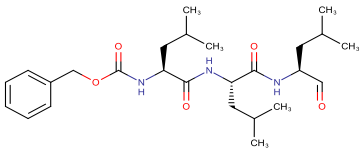
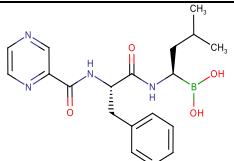


213

214 **Figure 2. Hit confirmation in DELFIA assay.** Hits from the AlphaLISA campaign were tested  
 215 in the DELFIA assay in duplicate in dose response (first point 100  $\mu$ M). Two controls were  
 216 included per plate and normalized as percent stimulation. Control 1 corresponds to the signal  
 217 obtained in the absence of inhibition (basal levels of ubiquitylated proteins corresponding to  
 218 100%), while Control 2 is the signal measured in wells treated with the proteasome inhibitor  
 219 MG132 (2  $\mu$ M). **A.** Bars represent the average percent stimulation per replicate. Average of signal  
 220 to background obtained per plate ( $S/B$ =average % stimulation Control 2 wells/average %  
 221 stimulation Control 1 wells) is indicated in bold for each replicate. **B.** Correlation of the pEC50s  
 222 recorded for each replicate. Compounds displaying a maximum percent stimulation higher than  
 223 131% were actives. In black, actives in two replicates ( $n=2$ ); in pink, actives in only one replicate  
 224 ( $n=1$ ); and in grey, compounds active in one replicate but whose curves could not be fitted in the  
 225 other replicate (non-adjusted NA). **C.** Correlation of the average pEC50s recorded in the  
 226 AlphaLISA and DELFIA assays per compound. Compounds labeled in black were active in more  
 227 than three replicates ( $n=2$  in AlphaLISA and/or DELFIA) and had a pEC50>4.5 in all replicates.  
 228 The black line indicates the perfect correlation ( $y=x$ ), while dotted lines represent  $\pm 1$  log difference  
 229 of perfect correlation. **D.** Correlation of the average pEC50s recorded in the AlphaLISA and whole  
 230 cell assays per compound. Labels are the same than in C.

231

232

Compound	Structure	Reported pEC50 whole cell 3D7A	UPS activity assays		Proteasome activity assays					
			pEC50 AlphaLISA	pEC50 DELFI A	pIC50 THP1			pIC50 <i>P. falciparum</i>		
					$\beta$ 5	$\beta$ 1	$\beta$ 2	$\beta$ 5	$\beta$ 1	$\beta$ 2
MG132		7.65	7.17 ± 0.04	7.41 ± 0.21	6.22 ± 0.01	5.25 ± 0.11	5.22 ± 0.11	6.86 ± 0.18	6.11 ± 0.02	6.72 ± 0.02
Bortezomib		7.05	7.95 ± 0.08	8.16 ± 0.05	7.29 ± 0.03	6.43 ± 0.20	5.56 ± 0.16	7.33 ± 0.26	<4*	<4

233 \* Some inhibition observed (~50% activity)

234 Table 1. Results for tool compound proteasome inhibitors in AMC assay for human THP1 and *P. falciparum* samples.

235

236 Figure 2C shows the correlation of the pEC50s found in the AlphaLISA and DELFIA assays.  
237 311 compounds were confirmed in the DELFIA assay in one or both replicates, revealing a  
238 confirmation rate of 57.1% with the AlphaLISA assay. Compounds active in more than two  
239 replicates in total (more than two active replicates in either AlphaLISA or DELFIA), and with a  
240 pEC50 higher than 4.5 (black) showed the best correlation, as they were the most reliable hits.  
241 Comparison of UPS and whole cell assays (Figure 2D) indicate that compounds are less potent  
242 in UPS assays, probably due to differences in the incubation times with the compounds, 1 hour  
243 vs. 48 hours respectively.

244 The results of both assays were used to select compounds for further studies. Thus, the 311  
245 compounds considered hits were tested in proteolytic activity assays of the proteasome which  
246 clearly differentiated two groups: compounds whose target is the proteasome (26S) and  
247 compounds that probably affect other UPS components upstream the proteasome (see graphical  
248 abstract).

249

### 250 ***Proteasome inhibitors***

251

252 Proteasome activity assays based on fluorescence readout were performed as described  
253 (22). Compounds showing autofluorescence at 460 nm were also tested in the Proteasome-Glo  
254 assay whose readout is luminescence. Proteasome-enriched fractions from *P. falciparum* extracts  
255 were used as proteasome source as previously described (22). All compounds were tested at  
256 single shot at 50  $\mu$ M in the chymotrypsin-like, caspase-like, and trypsin-like proteasome activity  
257 assays. Positive compounds were then subjected to dose response assays to assess their  
258 potency, in duplicate. Sixteen compounds were active in at least one of the activities tested and  
259 with an inhibition rate higher than 50%. Proteasome activity assays were also performed on  
260 human proteasome-enriched fractions from THP1 cells to assess selectivity. Proteasome  
261 inhibitors MG132 and bortezomib were included as controls in all experiments (Table 1). The  
262 identification of proteasome inhibitors was expected and validated the screening rational.

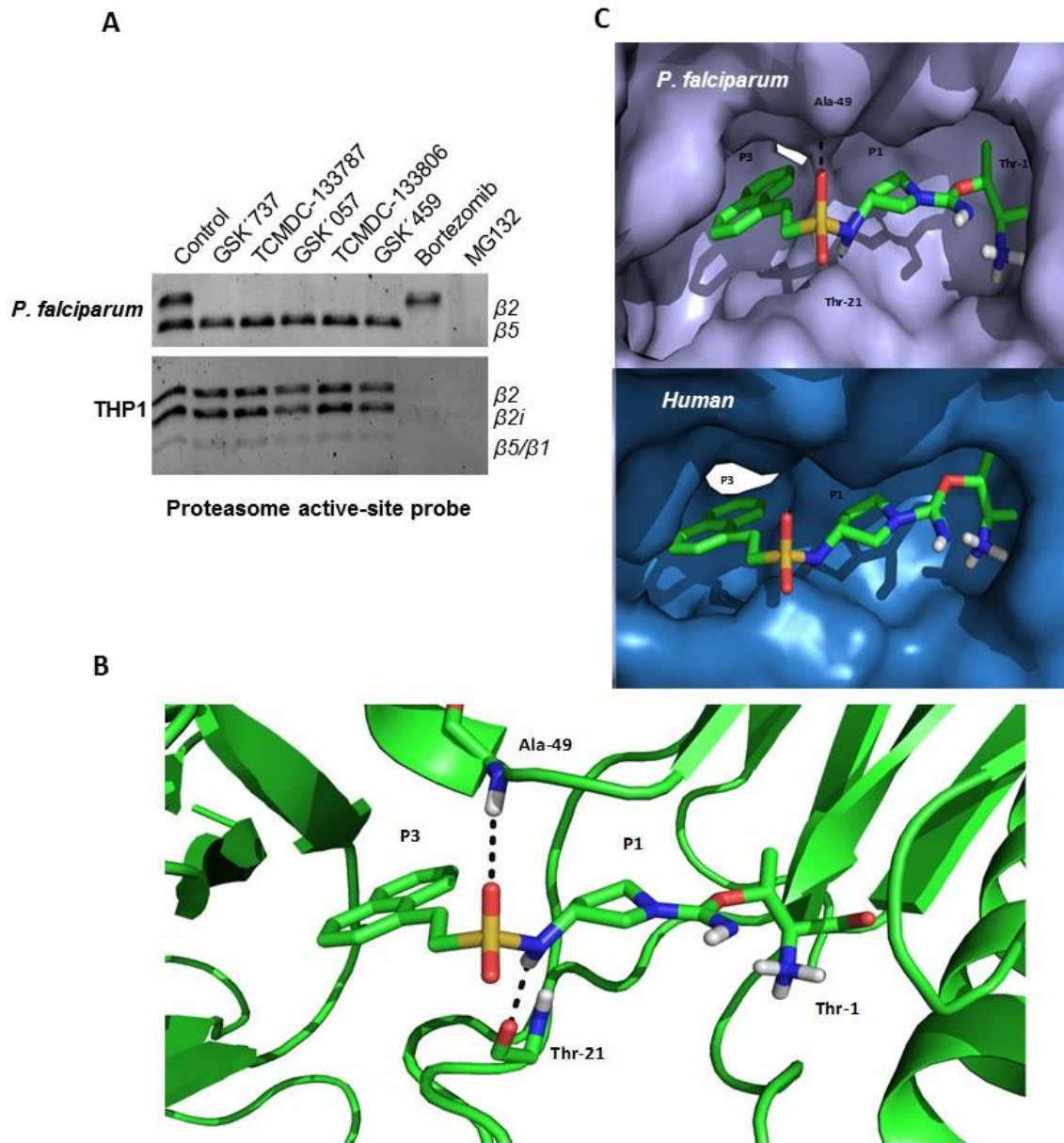
263 Most of the proteasome inhibitors found were not selective for the *P. falciparum* proteasome,  
264 which hampers further interest from a drug discovery point of view in malaria. However, results

265 showed that 6 compounds belonging to the same cluster with a cyanamide group were selective  
266 for the *P. falciparum* proteasome. Three of them belong to the TCAM set: TCMDC-133787,  
267 TCMDC-133806, and TCMDC-138496. All compounds inhibited the trypsin-like and caspase-like  
268 proteasome activities in *P. falciparum*, but not the chymotrypsin-like activity, while they had no  
269 effect on any human proteasome activities (Table 2). These compounds showed no cytotoxicity  
270 in the HepG2 assay. The Property Forecast Index (PFI) was calculated as a predictor of  
271 developability of compounds based on their physicochemical properties (23). Compounds with a  
272 PFI<8 are considered that met the “drug-like” criteria. PFI of cyanamide cluster is less than 8  
273 having a MW < 500, cLogP < 5, and a number of aromatic rings < 4.

274 A selection of analogs of these compounds were tested in the three proteasome activities of  
275 the parasite to better understand their structure-activity relationship (SAR) (data not shown).  
276 Compounds without the cyanamide group were inactive in the proteasome activity assays, which  
277 strongly suggests that this group is an essential component of the pharmacophore. SAR results  
278 also underlined the importance of other parts of the molecule, such as the sulfone group. The  
279 least potent compounds in the proteasome, such as GSK’459, do not have this group (Table 2),  
280 although in this case the decrease in potency is not reflected in whole cell activity. Activity  
281 improved when the position of the heteroatoms or the chiral center were changed, as in compound  
282 TCMDC-138496.

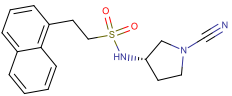
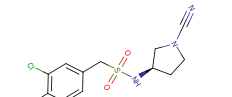
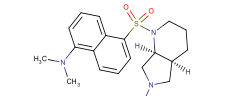
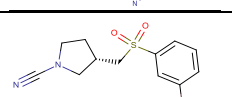
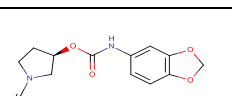
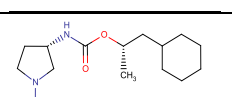
283 The subunit specificity of the proteasome inhibitors identified was assessed using the human  
284 active-site probe Me4BodipyFL-Ahx3Leu3VS (Figure 3A). This probe covalently reacts with all  
285 three  $\beta$  catalytic subunits in human proteasomes (24), but only with the trypsin-like ( $\beta$ 2) and  
286 chymotrypsin-like ( $\beta$ 5) in *P. falciparum* (11). The  $\beta$  subunits not bound to the inhibitors are labeled  
287 with the probe and then visualized by fluorescence. Treatment with our compounds caused the  
288 disappearance of the band corresponding to trypsin-like activity in *P. falciparum* but not in human  
289 fractions (Figure 3A). The human proteasome inhibitor bortezomib led to disappearance of all  
290 bands in human fractions, but only of the chymotrypsin-like band in *P. falciparum*, in agreement  
291 with the results reported in activity assays (Table 1). All bands in the human and parasite  
292 proteasomes were lost after treatment with the non-specific inhibitor MG132 (Figure 3A and Table  
293 1). These results confirmed the selectivity of our compounds against trypsin-like activity ( $\beta$ 2) in *P.*

294 *falciparum*, previously shown in the proteasome activity assays. Caspase-like activity could not  
 295 be confirmed, as it is not labeled by the probe in the *P. falciparum* proteasome (11, 13).



296

297 **Figure 3. Validation of proteasome inhibitors binding.** **A. Proteasome active-site probes.**  
 298 The proteasome active-site probe Me4BodipyFL-Ahx3Leu3VS was used reacting with the trypsin-  
 299 like ( $\beta 2$ ) and chymotrypsin-like ( $\beta 5$ ) proteasome activities in *P. falciparum* and with the three  $\beta$   
 300 catalytic subunits in THP1 in the absence of compounds. Proteasome-enriched fractions from *P.*  
 301 *falciparum* and THP1 cells were treated with compounds for 1 hour at 100  $\mu$ M. The probe was  
 302 then added labelling the proteasome active sites not previously bound to the compounds.  
 303 **B. Modelling of GSK'737 binding to *P. falciparum* and human proteasomes.** Proposed  
 304 binding mode of compound GSK'737 to *P. falciparum*  $\beta 2$  unit (trypsin-like activity). The compound  
 305 is predicted to bind covalently to the catalytic threonine residue, and to establish hydrogen bonds  
 306 with the backbone of residues Thr-21 and Ala-49. **C. Comparison of the binding modes in**  
 307 **human and *P. falciparum*** P1 and P3 sub pockets are highlighted.  
 308

Compound	PhysChem properties					Whole cell assays		UPS activity assays			Proteasome activity assays					
	Structure	cLogP	MW	Permeability	PFI	pEC50 3D7A	pEC50 Cytotox HepG2	pEC50 AlphaLISA	pEC50 DELFIA	n	pIC50 THP1			pIC50 <i>P. falciparum</i>		
											β5	β1	β2	β5	β1*	β2
GSK'737		2.4	329.4		6.4	6 ± 0.2	4.2 ± 0.0	5.2 ± 0.2	5.2 ± 0.1	4	<4	<4	<4	<4	6.1 ± 0.2	6.3 ± 0.1
TCMDC-133787		2.1	334.2	349	5.1	6.3 ± 0.1	4.3 ± 0.0	5.7 ± 0.2	4.6	3	<4	<4	<4	<4	6 ± 0.1	6.2 ± 0.2
GSK'057		3.5	384.5	480	7.3	6.3 ± 0.1	4.4 ± 0.2	5.0 ± 0.3	4.8 ± 0.3	4	<4	<4	<4	<4	6.4 ± 0.2	6.3 ± 0.1
TCMDC-133806		1.2	329.2	370	4.9	5.8 ± 0.1	<4	5.2 ± 0.1	4.6 ± 0.1	4	<4	<4	<4	<4	6.9 ± 0.3	6.8 ± 0.2
GSK'459		1.3	275.3		4	6.1 ± 0.2	<4	4.9	4.9 ± 0.5	3	<4	<4	<4	<4	5.3 ± 0.0	5.3 ± 0.1
TCMDC-138496		3.2	279.4		5.3	6.2 ± 0.1	4.1 ± 0.2	4.7 ± 0.1	4.5	3	<4	<4	<4	<4	5.9 ± 0.2	6.4 ± 0.3

309

\* No 100% inhibition (60%-80%)

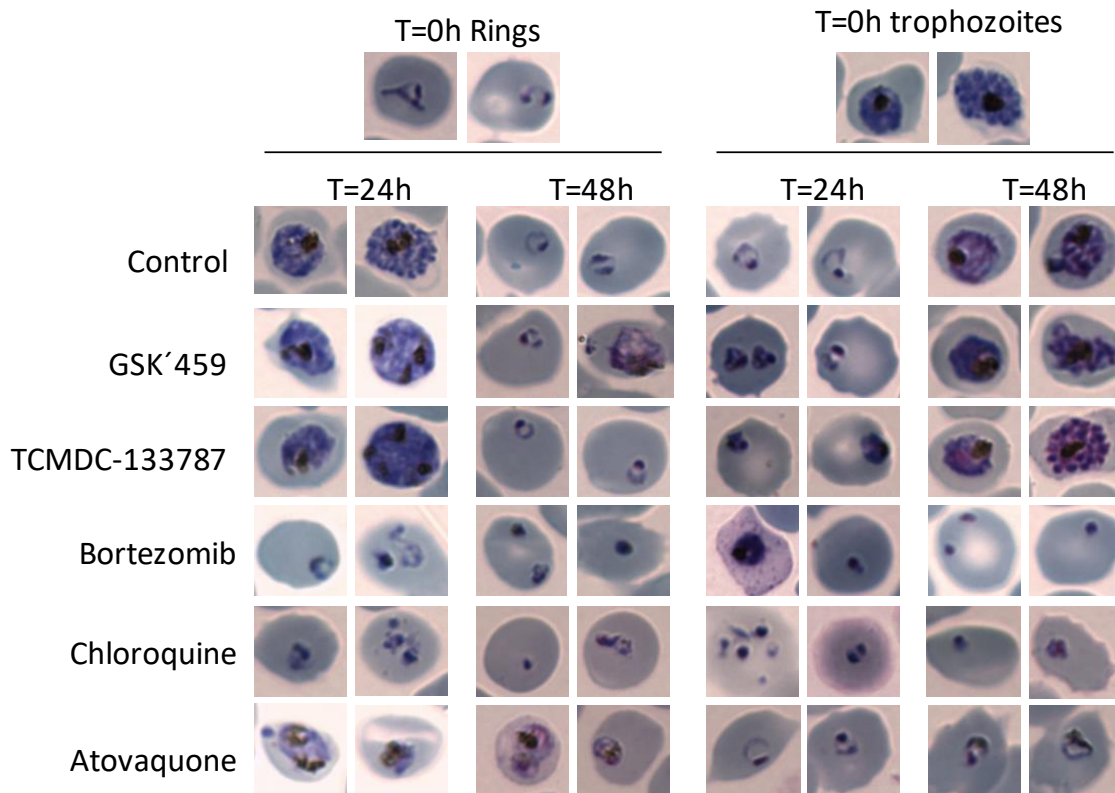
	Proteasome/Whole Cell Parasite	Proteasome/Cytotoxicity Human	cLogP	MW	Permeability	PFI
Green	> 6	< 4	≤ 3	≤ 350	≥ 100	≤ 6
Yellow	5-6	4-5	3-5	350-450	10-100	6-9
Red	< 4-5	> 5	≥ 5	≥ 450	≤ 10	≥ 9

310

Table 2. Summary of data for cyanamide proteasome inhibitors

311 To get some insight into the selectivity profile and mechanism of action of these compounds,  
312 molecular modeling studies were performed exploiting the recently published structural  
313 information about *P. falciparum* proteasome (12) and internal crystallographic complexes with  
314 other cyanamides and different serine and cysteine proteases (25). According to this information,  
315 these compounds could be acting as covalent ligands with the nitrile warhead. However, their  
316 selectivity towards  $\beta$ 1 and  $\beta$ 2 activities appears to point to a specific recognition mechanism.  
317 Based on this hypothesis, we modeled complexes of GSK'737 and TCMDC-133787 with the  $\beta$ 1,  
318  $\beta$ 2 and  $\beta$ 5 units of the human and *P. falciparum* proteasomes using a covalent docking workflow  
319 followed by manual refinement and energy minimization. In our proposed binding mode (Figure  
320 3B), the compounds are attached to the catalytic threonine residue after a reaction with the cyano  
321 group of the ligand, that is then interacting with the terminal amine group of the protein, similarly  
322 to other available complexes for cysteine proteases (25), in which the nitrogen atom adopts a role  
323 as a hydrogen bond acceptor. In our model, the P1 cavity would be partially occupied by the  
324 pyrrolidine ring as a proline analogue. This might explain the negligible activity of these  
325 compounds towards  $\beta$ 5 for both species, due to a possible requirement for a small hydrophobic  
326 residue (e.g. leucine) in that position for this catalytic unit (26). The different linkers (sulfonamide,  
327 methyl sulfone or carbamate) would establish hydrogen bond interactions with the backbone  
328 atoms of residues Ala-49 and Thr-21 (*P. falciparum*  $\beta$ 2 unit numbering scheme) in a similar  
329 manner to other known inhibitors such as WLW-vs derivatives (PDB ID 5FMG) (12) or bortezomib  
330 (PDB ID 5LF3) (27). The geometry imposed by the threonine-warhead complex would explain the  
331 different hydrogen bond patterns that the linkers could establish and, possibly, the potency drop  
332 for GSK'459. Finally, all compounds have a bulky, hydrophobic group (i.e. naphthalene  
333 derivatives, aryl halides, and 1,3 benzodioxol) that resembles, in different degrees, a tryptophan  
334 residue and that would be located in the P3 sub pocket. Recently, it has been discovered that the  
335 P3 sub pocket in *P. falciparum*  $\beta$  catalytic units, especially  $\beta$ 2, is significantly larger than that in  
336 their human homologues (Figure 3C), opening new opportunities to achieve selective inhibitors  
337 by introducing bulky groups into that position (e.g. tryptophan in WLL-vs inhibitor (12, 28)).  
338 According to our proposed binding mode, the presence of these groups in the reported  
339 compounds could be an example of such strategy and one of the reasons for their selectivity  
340 against the *P. falciparum* proteasome





342

343 **Figure 4. Effect of proteasome inhibitors identified on the intraerythrocytic parasite**  
 344 **stage.** Synchronized iRBCs with rings or mature trophozoites/schizonts were treated for 24 and  
 345 48 hours with compounds. Photographs of Giemsa-stained thin blood smears were taken to  
 346 observe the phenotype and the effect on parasite *in vitro* growth. Chloroquine and atovaquone  
 347 were included as controls of fast- and slow-acting compounds respectively with modes of action  
 348 unrelated to UPS inhibition.  
 349

350 To determine the effect on parasite growth of this family of trypsin-like and caspase-like  
 351 proteasome inhibitors, iRBCs synchronized in rings or mature trophozoites/schizonts were treated  
 352 for 24 and 48 hours with the compounds TCMDC-133787 and GSK'459. Bortezomib, chloroquine  
 353 and atovaquone were used as controls (Figure 4). Bortezomib is a human proteasome inhibitor  
 354 that inhibits the chymotrypsin-like activity. Treatment of parasites with bortezomib resulted in  
 355 parasite growth arrest in a similar way to chloroquine either in rings or mature forms. However,  
 356 treatment with our trypsin-like and caspase-like proteasome inhibitors, TCMDC-133787 and  
 357 GSK'459 did not prevent progression to the next parasite stage (Figure 4). In humans, *in*  
 358 *vitro* and *in vivo* protein degradation is significantly reduced only when either the trypsin-like or  
 359 caspase-like sites are inhibited together with the chymotrypsin-like sites (29). The same may  
 360 occur in the parasite. It has been reported that the most significant parasite killing results from co-  
 361 inhibition of the chymotrypsin-like activity with the trypsin-like or caspase-like proteasome

362 activities (12, 13). Co-inhibition allows for attenuating parasite growth at any point in the  
363 intraerythrocytic cycle. Chymotrypsin-like activity is essential for fast inhibition of growth being  
364 implicated in parasite schizogony, while inhibition of trypsin-like activity alone does not  
365 significantly affect parasite growth as it has been confirmed with our cyanamides. Parasitemia  
366 remained constant during the 48 hours tested, while in the control culture parasitemia increased  
367 more than 6-fold. They seemed to have no effect on trophozoites or early schizonts, but prevented  
368 increase in parasitemia, maybe because they affected merozoite egress, the invasion process,  
369 or early ring stages. The fact that not all parasite stages are equally sensitive to inhibition of the  
370 different proteolytic activities of the 20S core may suggest that each proteasome activity might be  
371 regulating a specific pool of ubiquitylated proteins (29).

372 On the other hand, some proteasome inhibitors can also react with other serine or cysteine  
373 proteases because the proteasome has a hydrolytic mechanism similar to those proteases (30).  
374 In fact, although cyanamides were selective for *P. falciparum* proteasome, it has previously been  
375 reported that they are inhibitors of different kinds of cathepsins, which are cysteine proteases. A  
376 cyanamide-based inhibitor analogue to TCMDC-133787 was reported by our colleagues at GSK  
377 as a novel human cathepsin C inhibitor for the treatment of neutrophil-dominated inflammatory  
378 diseases such as chronic obstructive pulmonary disease and cystic fibrosis (25). Selectivity for  
379 different cathepsins (cathepsins C, B, K, L, and S), all cysteine proteases, was achieved by  
380 changing different parts of the molecules. In the case of cyanamides identified here, the selectivity  
381 window in terms of cytotoxicity was higher than 100-fold in most cases. Further studies of the  
382 action of these compounds on different human cathepsins should be done to assess a good  
383 toxicological profile and to ensure the non-toxic effects *in vivo*.

384 As regards activity against other cysteine proteases of the parasite, it is known that *P.*  
385 *falciparum* has different families of cysteine proteases such as falcipains, which have been  
386 considered potential drug targets because they are involved in the hemoglobin degradation  
387 process. Treatment of cultured *P. falciparum* parasites with broadly active cysteine protease  
388 inhibitors such as leupeptin or E-64 causes the food vacuole to swell and fill with dark-staining  
389 material (31) due to accumulation of large amounts of undegraded hemoglobin, with maximum  
390 activity achieved in mature trophozoites and schizonts. Absence of a food vacuole defect in Figure

391 4 suggests that inhibition of cysteine proteases in this digestive organelle is not causing the  
392 inhibition of parasite growth.

393 All these results suggest that compounds belonging to the cyanamide cluster are good  
394 candidates to be administered in combination with other antimalarials such as artemisinin.  
395 Selective inhibitors acting upon the parasite trypsin-like activity have previously been shown to  
396 enhance killing by artemisinin of both sensitive and resistant parasites without host toxicity (12).  
397 In contrast to previously reported selective proteasome inhibitors, cyanamides are small  
398 molecules that are not peptide mimetics and have good PhysChem properties.

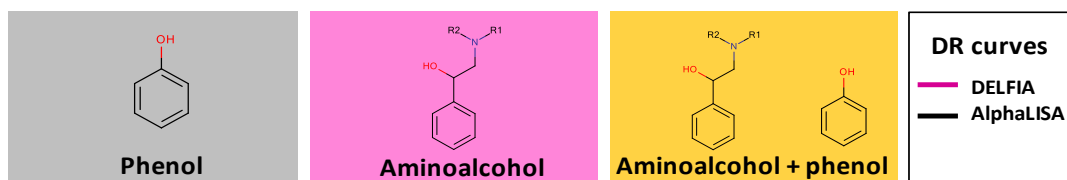
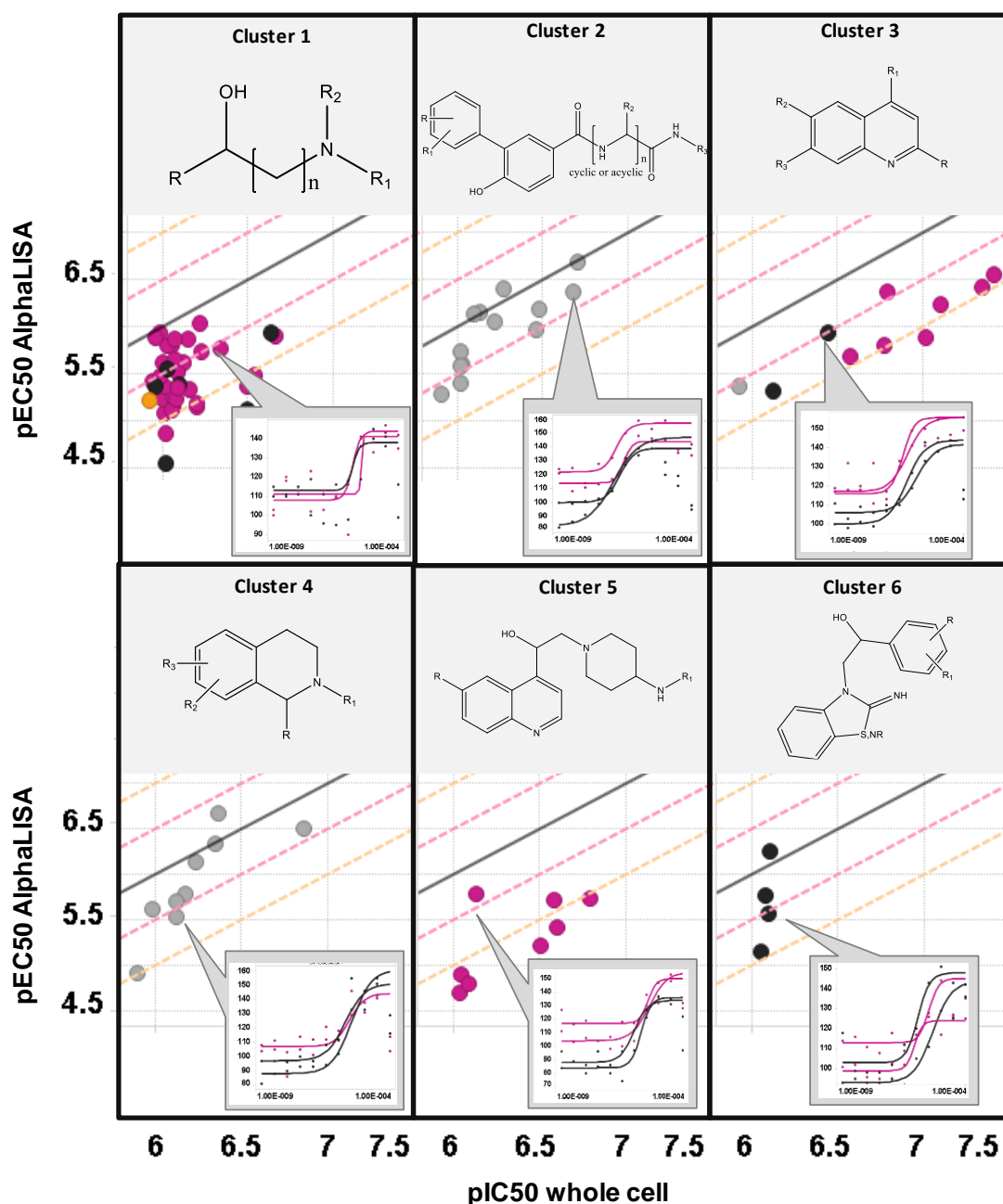
399

#### 400 ***Non-proteasome inhibitors***

401

402 In addition to proteasome inhibitors, our strategy has allowed the identification of compounds  
403 that increased ubiquitylated protein levels through other mechanisms that could be directly  
404 associated with parasite growth inhibition. This confirms published results showing that  
405 accumulation of ubiquitylated proteins can lead to parasite death (32).

406 295 compounds were inactive in all proteasome activity assays, forming the group of non-  
407 proteasome inhibitors (graphical abstract). Among them, 169 hits were active in the AlphaLISA  
408 and DELFIA assays in at least three replicates and with a pEC50 higher than 4.5 (Figure 2C,  
409 black dots). This restrictive selection criteria was applied to choose the best compounds of this  
410 group. In a first stage, the structures were clustered using a complete linkage hierarchical  
411 algorithm (21), which resulted in 64 chemical clusters, 36 of them singletons, with a wide variety  
412 of chemotypes. Further inspection revealed that most of them, irrespective of the cluster,  
413 contained a phenol group (such as phenol benzylamines), and/or were amino alcohols, including  
414 quinine and amino-phenyl-ethanol derivatives. Six were the most populated (82 compounds in  
415 total) clusters, with more than 3 members per cluster (Figure 5). The numbers of compounds  
416 within each cluster ranged from 38 in cluster 1 as the most populated and 4 in cluster 6 as the  
417 less populated. Clusters 1, 3 and 5 had with amino alcohols (pink dots). Most compounds in  
418 cluster 1 had a hydroxy group in benzyl position. The substitution of the amine could be aliphatic  
419 chains or aromatic rings.



420

421 **Figure 5. Non-proteasome inhibitors.** The six more populated clusters with their scaffolds  
 422 that share the compounds belonging to each cluster are presented. Graphs show the correlation  
 423 between the average pEC50 found in the UPS AlphaLISA assay and the pIC50 that inhibits  
 424 parasite *in vitro* growth (whole cell). The black line is the perfect correlation ( $y=x$ ), the pink and  
 425 orange dotted lines represent the  $\pm 0.5$  log and  $\pm 1$  log difference of perfect correlation respectively.  
 426 Compounds in grey have a phenol group, those in pink an amino alcohol group, and those in  
 427 orange both kinds of groups in their structure. Dose response curves for one of the compounds  
 428 belonging to each cluster are shown as examples. Percent stimulations recorded in the AlphaLISA  
 429 (black) and DELFIA (pink) assays for a representative of the cluster are plotted *versus* compound  
 430 concentration.

431 Clusters 3 and 5 shared a quinine scaffold. Moreover, cluster 5 had a long chain and was  
432 highly substituted in the right-hand side. The mechanism of action of quinine remains unclear, but  
433 the drug has been attributed an inhibitory role of hemozoin biocrystallization like chloroquine.  
434 However, some mutations have been found in the HECT E3 ligase *PfUT* (33) in quinine-resistant  
435 parasites (34), connecting the resistance with the UPS. The lower correlation seen with the whole  
436 cell assay here could point to an additional mechanism involving the UPS system of the parasite.

437 Clusters 2 and 4 contained compounds with the phenol group (Figure 5, grey dots). In  
438 addition, cluster 2 included structures similar to described protease inhibitors with benzamides  
439 substituted and an additional hydroxy group in para position, validating our approach. The  
440 interplay of phenols with the UPS has previously been reported in human cells. Natural phenolic  
441 compounds regulate the UPS during oxidative stress (35) and induce growth arrest or apoptosis  
442 probably by regulating the UPS. For example, compounds such as methyl gallate, gallic acid, and  
443 tannic acid increase ubiquitylated protein levels in treated human cells. They have an effect on  
444 the E1 conjugating enzyme activity and the 26S proteasome through their OH group, and also  
445 interact with other proteins such as protein S5a and DUBs USP47 and USP15 (36). The  
446 correlation of the pIC50s obtained in the UPS and in the whole cell assays may suggest that  
447 phenols present in the compounds could be affecting one or more components of the UPS.

448 Regarding the physicochemical profile, more than half the compounds showed a good PFI  
449 index and had no historical annotations of liabilities found in GSK internal databases (redox,  
450 promiscuity, reactivity, etc.), especially compounds belonging to clusters 1 (34/38), 3 (10/10), and  
451 4 (7/9). All compounds had less than 4 aromatic rings and most of them had a MW < 500 and a  
452 cLogP < 5. Regarding cytotoxicity, data in HepG2 showed that 77 of the 82 compounds were non-  
453 cytotoxic.

454 Figure 5 shows the correlation between AlphaLISA and *P. falciparum* 3D7A whole-cell  
455 assays pEC50s. The difference in pEC50 values was less than one for all of them, exhibiting  
456 almost the same potency in both assays despite the fact that treatment with compounds lasted  
457 only one hour. Phenols belonging to clusters 2 and 4 were near to perfect correlation, strongly  
458 suggesting that parasite growth and UPS inhibitions are related. Amino alcohols present in  
459 clusters 3 and 5 also showed a good correlation but, in all cases, compounds were more potent  
460 in the whole cell assay, possibly indicating that there are other targets involved in their mode of

461 action or that more time is needed for compounds to exert their action. Some dose response  
462 curves are presented in Figure 5 as an example of the results found for each cluster.

463 Little is known about components of the UPS in *P. falciparum*. Future identification of the  
464 proteins targeted by these non-proteasome inhibitor compounds could reveal novel, validated,  
465 tractable and selective targets which could be used in new drug discovery programs. Further  
466 studies, like chemogenomic or proteomic methods (e.g. global shift thermal profiling) among  
467 others, are required to identify which targets are being hit by the inhibitors found.

468

## 469 **Conclusion**

470

471 Results from the screening campaign shown here revealed compounds hitting different  
472 targets within the UPS pathway. They represent excellent starting points for drug discovery  
473 programs, particularly compounds belonging to the proteasome inhibitors, as the target they are  
474 hitting has been identified. Moreover, non-proteasome inhibitors described could be used as tools  
475 to identify new tractable antimalarial targets.

476

## 477 **Materials and methods**

478

### 479 ***P. falciparum* cultures**

480 *P. falciparum* 3D7A strain from the Malaria Research and Reference Reagent Resource  
481 Center (MR4) was used to perform all assays reported. Parasites were grown in T150 flasks with  
482 fresh red blood cells (RBCs) at hematocrit 1% (volume percentage of RBCs) as described in (31).

483

### 484 ***Preparation of assay plates***

485 Compounds were dissolved in 100% DMSO. Final DMSO concentration in the assays was  
486 1%. AlphaLISA assay plates (Greiner 1536-well white plates) were prepared with compounds by  
487 adding 20 nL of each compound per well with an Echo dispenser, except for columns 11 and 12,  
488 which were filled with 20 nL of DMSO, and columns 35 and 36, which were left empty. 200 nL of  
489 each compound were added to 384-well flat bottom black plates for DELFIA assays, while 40 nL  
490 were dispensed to 384-well low volume black plates for proteasome assays. Columns 6 and 18

491 were left empty. For single shot assays, final compound concentration in the assay was 10  $\mu$ M in  
492 AlphaLISA and 50  $\mu$ M in the proteasome assays. For dose response determinations in any of the  
493 assays described, the highest concentration was 100  $\mu$ M, and 11 points diluted 1:3 in DMSO  
494 were tested in all the assays performed by duplicate.

495

#### 496 ***Purification of iRBCs with mature trophozoites/schizonts***

497 Purified, highly synchronized *P. falciparum*-infected red blood cells (iRBCs) with mature forms  
498 were required to perform the HTS campaign. The previously described protocol was used for this  
499 purpose (37). As control of inhibition, part of the culture was treated with 1.5  $\mu$ M of MG132  
500 dissolved in DMSO. Culture was dispensed into AlphaLISA and DELFIA plates as described in  
501 each section. All this experimental work was carried out under biosafety level 3 procedures.

502

#### 503 ***TUBE-AlphaLISA and DELFIA assays***

504 A Multidrop Combi liquid handler (Thermo Electron Corporation) was used for each reagent  
505 addition to assay plates. The protocol was followed as described by Mata-Cantero et al (17).

506

#### 507 ***Data analysis***

508 Data were normalized to percentage of stimulation using the following equation:

$$509 \quad \% \text{ Stimulation}(x) = \frac{R_x}{|R_{Ctrl1}|} * 100$$

510  $R_x$  is the assay response measured for compound X, while  $R_{Ctrl1}$  is calculated as the average  
511 of control 1 (columns with 1% DMSO) in the same plate of compound X. Data and assay  
512 performance statistics, such as signal to background ratio (S/B), robust standard deviation (SD),  
513 and coefficient of variation (CV= (SD/average)\*100) were calculated using ActivityBase XE  
514 (IDBS) templates. Robust cut-offs at robust mean + 3\*SD of Control 1 (estimated through a robust  
515 algorithm) (38) were used to mark the hits. Before that, patterns present in the plates were  
516 detected and removed using an in-house developed algorithm (20). pEC50 values  
517 (pEC50 =  $-\log_{10}(\text{EC50})$ ) were obtained with ActivityBase XE non-linear regression bundle. Data  
518 visualization and further analysis were performed using TIBCO Spotfire 3.2 software and  
519 Microsoft Excel.

520

521 ***Selection criteria and data mining***

522 For single shot experiments, hits had a response above the statistical cut-off (robust  
523 mean + 3\*SD response of Control 1) of each replicate. In AlphaLISA and DELFIA dose response  
524 assays, compounds with a maximum asymptote higher than 131% were considered active  
525 compounds (actives). This is based on the response and standard deviation obtained in the  
526 experiments calculated as stated above. Compounds with pEC50 values lower than 4 (> 100 µM)  
527 were considered inactive. GSK proprietary compound screening databases were queried for  
528 historical data of the hits obtained. For proteasome activity assays described in a following  
529 section, compounds showing a maximum percentage of inhibition higher than 50% in at least one  
530 proteasome activity were considered actives.

531

532 ***Proteasome-enriched fractions***

533 The protocol described by Kisselev et al (22) was adapted to obtain proteasome-enriched  
534 fractions present in purified *P. falciparum* cells and THP1 crude extracts. Briefly, *P. falciparum*  
535 cultures were synchronized with 5% sorbitol (w/v) and scaled up for five days. Culture was  
536 harvested by centrifugation at 700 g for 5 minutes, and parasites were isolated by breaking RBCs  
537 with 0.01% saponin (w/v) as previously described. At this point, parasite and THP1 cell were  
538 equally processed. Cells were resuspended in sucrose buffer (50 mM Tris buffer pH 7.5, 5 mM  
539 MgCl<sub>2</sub>, 1 mM EDTA, 50 mM NaCl, 250 mM sucrose, 2 mM ATP, 1 mM DTT) and lysed by nitrogen  
540 cavitation for 15 minutes (110 bar of 1500 psi). Lysates were centrifuged at 20,000 g for  
541 30 minutes at 4°C, and supernatants containing soluble protein were subjected to an  
542 ultracentrifugation step at 300,000 g for 2 hours at 4°C. The resulting proteasome-containing  
543 pellets were resuspended in sucrose buffer and left on ice for 30 minutes to complete  
544 solubilization. Samples were centrifuged for 10 minutes at 20,000 g to remove insoluble material.  
545 Proteins contained in supernatant, the proteasome-enriched fraction, were measured using the  
546 Bradford method.

547

548 ***Proteasome activity assays***

549 Proteasome activities were assayed with fluorogenic or luminescence peptide substrates  
550 using previously described methods (22, 39) or the Proteasome-Glo assays (Promega)



551 respectively. In fluorescence assays, proteasome-enriched fractions from *P. falciparum* cells were  
552 dissolved in sucrose buffer at 0.1 mg/mL to measure the three proteasome activities. THP1  
553 proteasome-enriched fractions were adjusted to 0.1 mg/mL for the chymotrypsin-like activity and  
554 to 0.2 mg/mL for the caspase-like and trypsin-like activities. 4  $\mu$ L of proteasome-enriched fractions  
555 at the required concentration were added to compounds and incubated for 1 hour (384-well, low  
556 volume plates). Then, 4  $\mu$ L of peptides 100  $\mu$ M Suc-LLVY-AMC (Sigma), 200  $\mu$ M Z-Leu-Leu-Glu-  
557 AMC (Sigma) or 200  $\mu$ M Ac-RLR-AMC (Boston) in assay buffer (50 mM Tris buffer pH 7.5, 5 mM  
558  $MgCl_2$ , 1 mM EDTA, 50 mM NaCl, 1 mM DTT, 2 mM ATP, BSA 0.1 mg/ml) were added to the  
559 plates to measure the chymotrypsin-like, caspase-like or trypsin-like proteasome activities  
560 respectively. Proteasome inhibitors epoxomicin and MG132 at 10  $\mu$ M were included as controls.  
561 In the Proteasome-Glo assay, proteasome-enriched fractions were assayed in HEPES buffer  
562 (10 mM HEPES, 1 mM DTT, 2 mM ATP, BSA 0.1 mg/ml) following manufacturer protocols.  
563 Proteasome concentration for *P. falciparum* was kept at 0.1 mg/mL, while THP1 proteasome was  
564 used at 0.05 mg/mL for chymotrypsin-like and trypsin-like activities, and at 0.1 mg/mL for  
565 caspase-like activity. Volumes and order of addition were the same as in the fluorescence assay.  
566 Fluorescence ( $\lambda_{ex/em} = 380/460$  nm) or luminescence were measured in the Envision plate reader  
567 (Perkin Elmer). For dose response experiments, the first compound concentration tested was  
568 100  $\mu$ M diluting the compounds 1:3 in DMSO (final DMSO concentration, 1%).

569

#### 570 ***Proteasome active-site probes***

571 For all proteasome labeling experiments, the active-site probe Me4BodipyFL-Ahx3Leu3VS  
572 (UbiQ) was used at a final concentration of 500 nM in sucrose buffer. THP1 (20  $\mu$ g) or *P.*  
573 *falciparum* (10  $\mu$ g) proteasome-enriched fractions were incubated with compounds at 100  $\mu$ M, or  
574 DMSO as control, for 1 hour in sucrose buffer. The active-site probe was added to proteasome  
575 enriched fractions previously treated with DMSO or compounds and incubated for 2 hours at RT.  
576 Samples were then denatured by addition of Laemmli sample buffer, boiled for 10 minutes and  
577 run on a 15% SDS-PAGE gel. Bands were visualized using the fluorescein channel in a Chemidoc  
578 reader (Biorad) ( $\lambda_{ex/em} = 480/530$  nm).

579

#### 580 ***Whole cell inhibition assay***

581 The parasite growth inhibition assay was performed using the standard <sup>3</sup>H-hypoxanthine  
582 incorporation method. This assay relies on parasite incorporation of labeled hypoxanthine that is  
583 proportional to *P. falciparum* growth (40).

584

#### 585 ***Parasite inhibition phenotype***

586 *P. falciparum* cultures were synchronized in schizonts by performing 70% Percoll gradient  
587 centrifugation. Next day, culture in rings at 2% parasitemia and 2% hematocrit was treated with  
588 compounds at 10 times their IC50s in the whole cell assay, 0.01 μM atovaquone, 0.25 μM  
589 chloroquine, 1 μM bortezomib (Selleckchem), 5 μM TCMDC-133787, and 15 μM GSK'459, at a  
590 final DMSO concentration of 0.5%. After 24 hours, parasitemia was quantified and photographs  
591 were taken of Giemsa-stained thin blood smears. The same experiment was carried out treating  
592 the parasites in mature trophozoites/schizonts.

593

#### 594 ***HepG2 cytotoxicity assay***

595 The acute cytotoxic effect of compounds administered to growing human liver-derived  
596 HepG2 cells (ATCC HB-8065) was determined using the luminescence assay previously  
597 described (41).

598

#### 599 ***Molecular modeling***

600 The structure of the three catalytic β1, β2, and β5 subunits of the *P. falciparum* proteasome  
601 were obtained from the cryo-EM derived structure (PDB ID 5FMG) (12, 28), while human subunits  
602 were obtained from the apo X-ray crystal (4R3O) (42). The Schrodinger 2017-3 suite was used  
603 to pre-process protein structure, model the missing side chains, and assign optimal protonation  
604 states. 3D models for the compounds were generated with Ligprep, followed by a conformational  
605 analysis to generate low-energy states for input in the docking protocol. The covalent docking  
606 module in Maestro was used to generate and score different poses with a covalent bond between  
607 the cyano group and the oxygen in the Thr-1 side chain (nucleophilic addition to a triple bond).  
608 The resulting poses for the 6 systems (β1, β2, and β5 for human and *P. falciparum*) were manually  
609 analyzed and corrected based on information from internal crystal complexes with other cysteine

610 proteases, and the final complexes were energy-minimized to a final RMSD from the original  
611 structure of 0.3 Å.

612

613

#### 614 **Acknowledgements**

615 Human RBCs were supplied by the Blood Transfusion Center of CAM (Madrid, Spain) and Banc  
616 de Sang i Teixits (Barcelona, Spain). Human biological samples were sourced ethically, and their  
617 research use complied with the terms of the informed consent under an IRB/EC approved  
618 protocol. We also thank Jim Brown for critically review of the manuscript. GSK has funded this  
619 work.

620

#### 621 **References**

622

- 623 1. **WHO**. 2018. World Malaria Report 2018.
- 624 2. **Gamo FJ**. 2014. Antimalarial drug resistance: new treatments options for Plasmodium.  
625 Drug Discov Today Technol **11**:81-88.
- 626 3. **Ng CL, Fidock DA, Bogyo M**. 2017. Protein Degradation Systems as Antimalarial  
627 Therapeutic Targets. Trends Parasitol **33**:731-743.
- 628 4. **Aminake MN, Arndt HD, Pradel G**. 2012. The proteasome of malaria parasites: A multi-  
629 stage drug target for chemotherapeutic intervention? Int J Parasitol Drugs Drug Resist  
630 **2**:1-10.
- 631 5. **Komander D**. 2009. The emerging complexity of protein ubiquitination. Biochem Soc  
632 Trans **37**:937-953.
- 633 6. **Bedford L, Paine S, Sheppard PW, Mayer RJ, Roelofs J**. 2010. Assembly, structure, and  
634 function of the 26S proteasome. Trends Cell Biol **20**:391-401.
- 635 7. **Schmidt M, Finley D**. 2014. Regulation of proteasome activity in health and disease.  
636 Biochim Biophys Acta **1843**:13-25.

- 637 8. **Xolalpa W, Perez-Galan P, Rodriguez MS, Roue G.** 2013. Targeting the ubiquitin  
638 proteasome system: beyond proteasome inhibition. *Curr Pharm Des* **19**:4053-4093.
- 639 9. **Mata-Cantero L, Lobato-Gil S, Aillet F, Rodriguez MS.** 2015. The ubiquitin proteasome  
640 system (UPS) as a cancer drug target: emerging mechanisms and therapeutics, p 225–  
641 264. *In* Wondrak SL (ed), *The ubiquitin proteasome system (UPS) as a cancer drug target:*  
642 *emerging mechanisms and therapeutics* doi:10.1007/ 978-94-017-9421-3-11 Springer  
643 Science + Business Media.
- 644 10. **Tschan S, Brouwer AJ, Werkhoven PR, Jonker AM, Wagner L, Knittel S, Aminake MN,**  
645 **Pradel G, Joanny F, Liskamp RM, Mordmuller B.** 2013. Broad-spectrum antimalarial  
646 activity of peptido sulfonyl fluorides, a new class of proteasome inhibitors. *Antimicrob*  
647 *Agents Chemother* **57**:3576-3584.
- 648 11. **Li H, Ponder EL, Verdoes M, Asbjornsdottir KH, Deu E, Edgington LE, Lee JT, Kirk CJ,**  
649 **Demo SD, Williamson KC, Bogyo M.** 2012. Validation of the proteasome as a therapeutic  
650 target in Plasmodium using an epoxyketone inhibitor with parasite-specific toxicity.  
651 *Chem Biol* **19**:1535-1545.
- 652 12. **Li H, O'Donoghue AJ, van der Linden WA, Xie SC, Yoo E, Foe IT, Tilley L, Craik CS, da**  
653 **Fonseca PC, Bogyo M.** 2016. Structure- and function-based design of Plasmodium-  
654 selective proteasome inhibitors. *Nature* **530**:233-236.
- 655 13. **Li H, van der Linden WA, Verdoes M, Florea BI, McAllister FE, Govindaswamy K, Elias**  
656 **JE, Bhanot P, Overkleeft HS, Bogyo M.** 2014. Assessing subunit dependency of the  
657 Plasmodium proteasome using small molecule inhibitors and active site probes. *ACS*  
658 *Chem Biol* **9**:1869-1876.
- 659 14. **Xie SC, Gillett DL, Spillman NJ, Tsu C, Luth MR, Otilie S, Duffy S, Gould AE, Hales P,**  
660 **Seager BA, Charron CL, Bruzzese F, Yang X, Zhao X, Huang SC, Hutton CA, Burrows JN,**  
661 **Winzeler EA, Avery VM, Dick LR, Tilley L.** 2018. Target Validation and Identification of

- 662 Novel Boronate Inhibitors of the Plasmodium falciparum Proteasome. J Med Chem  
663 **61**:10053-10066.
- 664 15. **Mata-Cantero L, Azkargorta M, Aillet F, Xolalpa W, LaFuente MJ, Elortza F, Carvalho**  
665 **AS, Martin-Plaza J, Matthiesen R, Rodriguez MS.** 2016. New insights into host-parasite  
666 ubiquitin proteome dynamics in P. falciparum infected red blood cells using a TUBEs-MS  
667 approach. J Proteomics **139**:45-59.
- 668 16. **Artavanis-Tsakonas K, Weihofen WA, Antos JM, Coleman BI, Comeaux CA, Duraisingh**  
669 **MT, Gaudet R, Ploegh HL.** 2010. Characterization and structural studies of the  
670 Plasmodium falciparum ubiquitin and Nedd8 hydrolase UCHL3. J Biol Chem **285**:6857-  
671 6866.
- 672 17. **Mata-Cantero L, Cid C, Gomez-Lorenzo MG, Xolalpa W, Aillet F, Martin JJ, Rodriguez**  
673 **MS.** 2015. Development of two novel high-throughput assays to quantify ubiquitylated  
674 proteins in cell lysates: application to screening of new anti-malarials. Malar J **14**:200.
- 675 18. **Gamo FJ, Sanz LM, Vidal J, de Cozar C, Alvarez E, Lavandera JL, Vanderwall DE, Green**  
676 **DV, Kumar V, Hasan S, Brown JR, Peishoff CE, Cardon LR, Garcia-Bustos JF.** 2010.  
677 Thousands of chemical starting points for antimalarial lead identification. Nature  
678 **465**:305-310.
- 679 19. **Kreidenweiss A, Kremsner PG, Mordmuller B.** 2008. Comprehensive study of  
680 proteasome inhibitors against Plasmodium falciparum laboratory strains and field  
681 isolates from Gabon. Malar J **7**:187.
- 682 20. **Coma I, Herranz J, Martin J.** 2009. Statistics and decision making in high-throughput  
683 screening. Methods Mol Biol **565**:69-106.
- 684 21. **Leach A, Guillet V.** 2007. Selecting Diverse Sets of Compounds: Hierarchical Clustering.  
685 Springer: Dordrecht, Netherlands, An Introduction to Chemoinformatics.
- 686 22. **Kisselev AF, Goldberg AL.** 2005. Monitoring activity and inhibition of 26S proteasomes  
687 with fluorogenic peptide substrates. Methods Enzymol **398**:364-378.

- 688 23. **Young RJ, Green DV, Luscombe CN, Hill AP.** 2011. Getting physical in drug discovery II:  
689 the impact of chromatographic hydrophobicity measurements and aromaticity. Drug  
690 Discov Today **16**:822-830.
- 691 24. **Berkers CR, Leestemaker Y, Schuurman KG, Ruggeri B, Jones-Bolin S, Williams M, Ovaa**  
692 **H.** 2012. Probing the specificity and activity profiles of the proteasome inhibitors  
693 bortezomib and delanzomib. Mol Pharm **9**:1126-1135.
- 694 25. **Laine D, Palovich M, McClelland B, Petitjean E, Delhom I, Xie H, Deng J, Lin G, Davis R,**  
695 **Jolit A, Nevins N, Zhao B, Villa J, Schneck J, McDevitt P, Midgett R, Kmett C, Umbrecht**  
696 **S, Peck B, Davis AB, Bettoun D.** 2011. Discovery of novel cyanamide-based inhibitors of  
697 cathepsin C. ACS Med Chem Lett **2**:142-147.
- 698 26. **Rawlings ND, Barrett AJ, Bateman A.** 2011. MEROPS: the database of proteolytic  
699 enzymes, their substrates and inhibitors. Nucleic acids research **40**:D343-D350.
- 700 27. **Schrader J, Henneberg F, Mata RA, Tittmann K, Schneider TR, Stark H, Bourenkov G,**  
701 **Chari A.** 2016. The inhibition mechanism of human 20S proteasomes enables next-  
702 generation inhibitor design. Science **353**:594-598.
- 703 28. **Li H, Bogyo M, da Fonseca PC.** 2016. The cryo-EM structure of the Plasmodium  
704 falciparum 20S proteasome and its use in the fight against malaria. FEBS J **283**:4238-  
705 4243.
- 706 29. **Kisselev AF, Callard A, Goldberg AL.** 2006. Importance of the different proteolytic sites  
707 of the proteasome and the efficacy of inhibitors varies with the protein substrate. J Biol  
708 Chem **281**:8582-8590.
- 709 30. **Kisselev AF, Goldberg AL.** 2001. Proteasome inhibitors: from research tools to drug  
710 candidates. Chem Biol **8**:739-758.
- 711 31. **Prasad R, Atul, Kolla VK, Legac J, Singhal N, Navale R, Rosenthal PJ, Sijwali PS.** 2013.  
712 Blocking Plasmodium falciparum development via dual inhibition of hemoglobin  
713 degradation and the ubiquitin proteasome system by MG132. PLoS One **8**:e73530.

- 714 32. **Bridgford JL, Xie SC, Cobbold SA, Pasaje CFA, Herrmann S, Yang T, Gillett DL, Dick LR,**  
715 **Ralph SA, Dogovski C, Spillman NJ, Tilley L.** 2018. Artemisinin kills malaria parasites by  
716 damaging proteins and inhibiting the proteasome. *Nat Commun* **9**:3801.
- 717 33. **Sanchez CP, Rotmann A, Stein WD, Lanzer M.** 2008. Polymorphisms within PfMDR1  
718 alter the substrate specificity for anti-malarial drugs in *Plasmodium falciparum*. *Mol*  
719 *Microbiol* **70**:786-798.
- 720 34. **Sanchez CP, Liu CH, Mayer S, Nurhasanah A, Cyrklaff M, Mu J, Ferdig MT, Stein WD,**  
721 **Lanzer M.** 2014. A HECT ubiquitin-protein ligase as a novel candidate gene for altered  
722 quinine and quinidine responses in *Plasmodium falciparum*. *PLoS Genet* **10**:e1004382.
- 723 35. **Chang TL, Lin SW, Wu SL, Hong CM.** 2013. Regulation of ubiquitin and 26S proteasome  
724 mediated by phenolic compounds during oxidative stress. *J Nutr Biochem* **24**:1970-1981.
- 725 36. **Chang TL, Chiang HY, Shena JY, Lin SW, Tsai PJ.** 2015. Phenolic compounds stage an  
726 interplay between the ubiquitin–proteasome system and ubiquitin signal autophagic  
727 degradation for the ubiquitin-based cancer chemoprevention. *Journal of Functional*  
728 *Foods* **17**:857-871.
- 729 37. **Mata-Cantero L, Lafuente MJ, Sanz L, Rodriguez MS.** 2014. Magnetic isolation of  
730 *Plasmodium falciparum* schizonts iRBCs to generate a high parasitaemia and  
731 synchronized in vitro culture. *Malar J* **13**:112.
- 732 38. **Analytical Methods Committee.** 1989. Robust Statistics—How Not to Reject Outliers, p  
733 1693–1697. *In Analyst* (ed), vol 114.
- 734 39. **Rivett AJ, Savory PJ, Djaballah H.** 1994. Multicatalytic endopeptidase complex:  
735 proteasome. *Methods Enzymol* **244**:331-350.
- 736 40. **de Cozar C, Caballero I, Colmenarejo G, Sanz LM, Alvarez-Ruiz E, Gamo FJ, Cid C.** 2016.  
737 Development of a Novel High-Density [3H]Hypoxanthine Scintillation Proximity Assay To  
738 Assess *Plasmodium falciparum* Growth. *Antimicrob Agents Chemother* **60**:5949-5956.

- 739 41. **Crouch SPM KR, Slater KJ, Fletcher J.** 1993. the use of ATP bioluminescence as a  
740 measure of cell-proliferation and cytotoxicity. *J Immunol Methods* **160**:81–88.
- 741 42. **Harshbarger W, Miller C, Diedrich C, Sacchetti J.** 2015. Crystal structure of the human  
742 20S proteasome in complex with carfilzomib. *Structure* **23**:418-424.
- 743



